

Supplementary information:

Tramp element drag on grain boundaries controlling microstructural and residual stress equilibration in copper thin-films

Charlotte Cui^{1§}, Rahulkumar Sinojiya^{1§}, Bernhard Sartory¹, Michael Tkadletz², Michael Reisinger³, Johannes Zechner⁴, Werner Robl⁵, Roland Brunner^{1*}

¹ Materials Center Leoben Forschung GmbH, Vordemberger Straße 12, AT 8700 Leoben, Austria

² Christian Doppler Laboratory for Sustainable Hard Coatings at the Department of Materials Science, Montanuniversität Leoben, Franz-Josef-Straße 18, 8700 Leoben, Austria

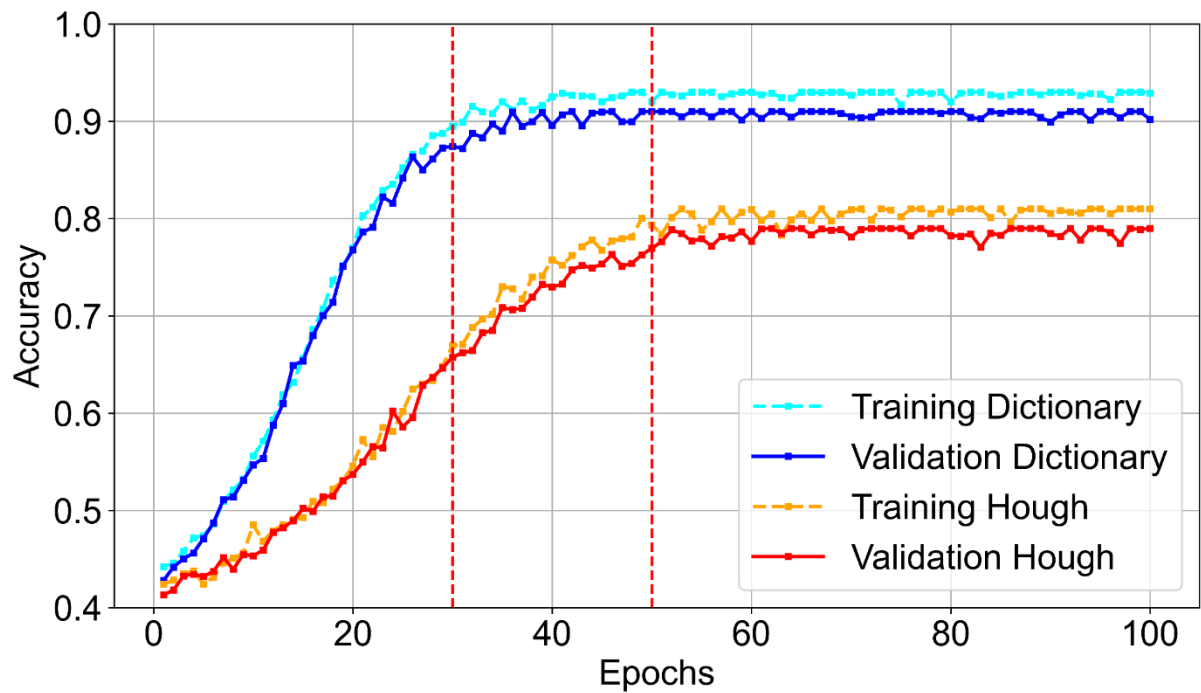
³ Kompetenzzentrum für Automobil- und Industrielektronik GmbH, Europastraße 8, 9524 Villach, Austria

⁴ Infineon Technologies Austria, Siemensstraße 2, 9500 Villach, Austria

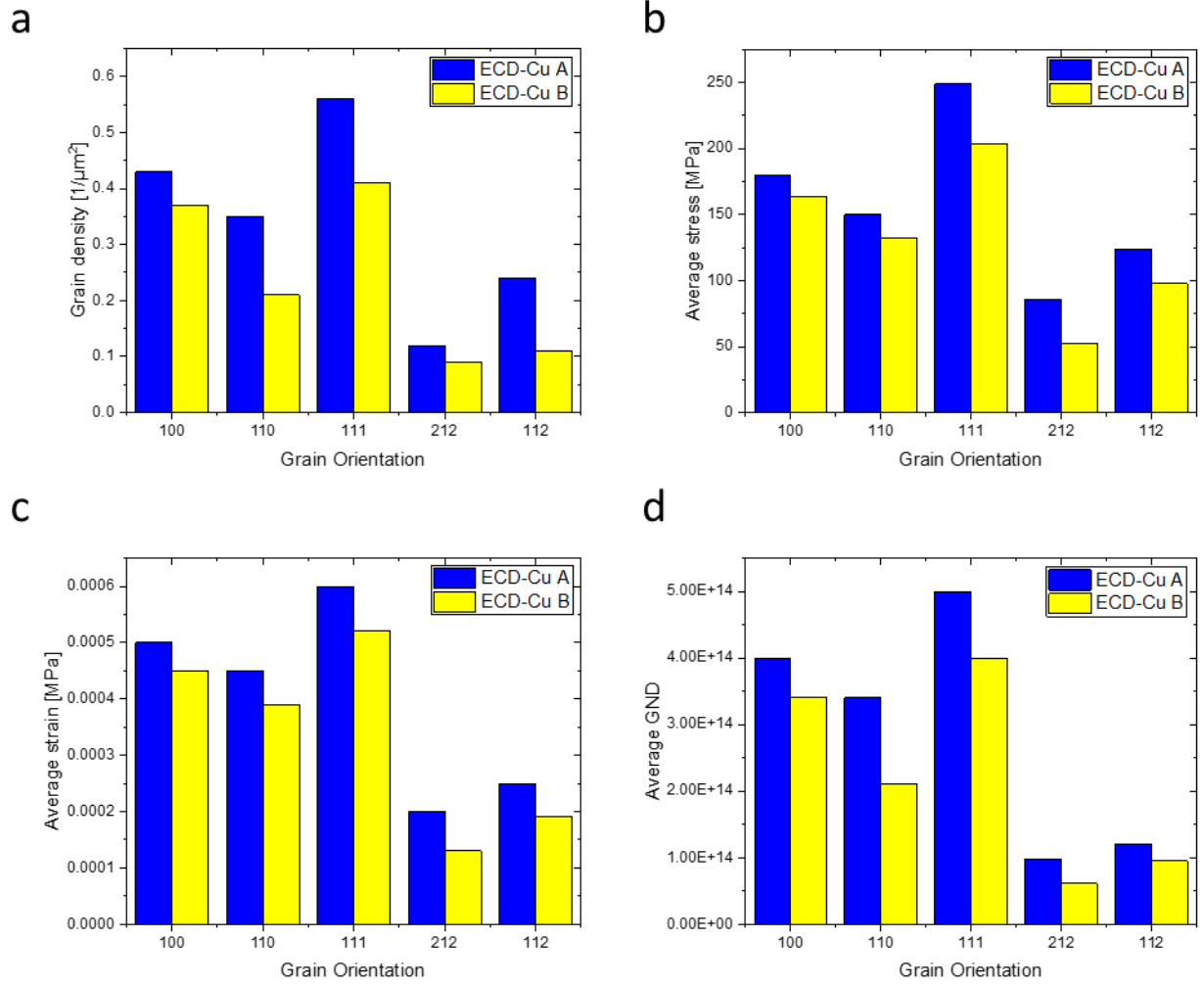
⁵ Infineon Technologies AG, Wernerwerkstraße 2, 93049 Regensburg, Germany

*Corresponding author: roland.brunner@mcl.at

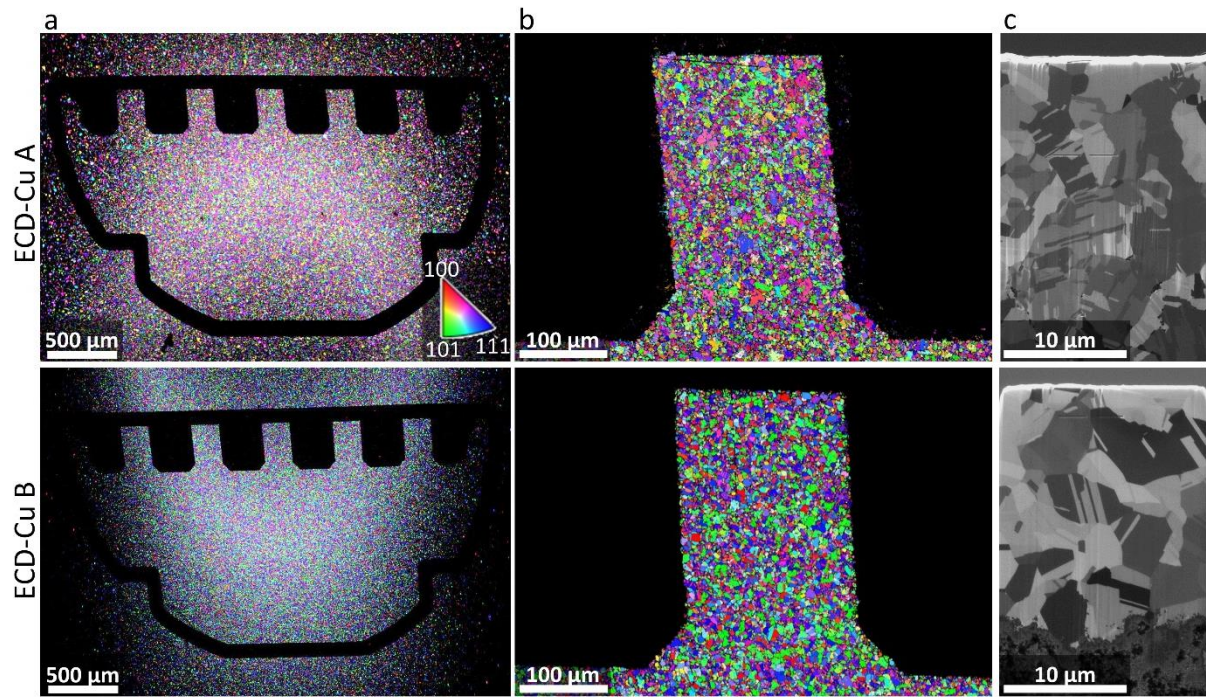
[§] authors contributed equally



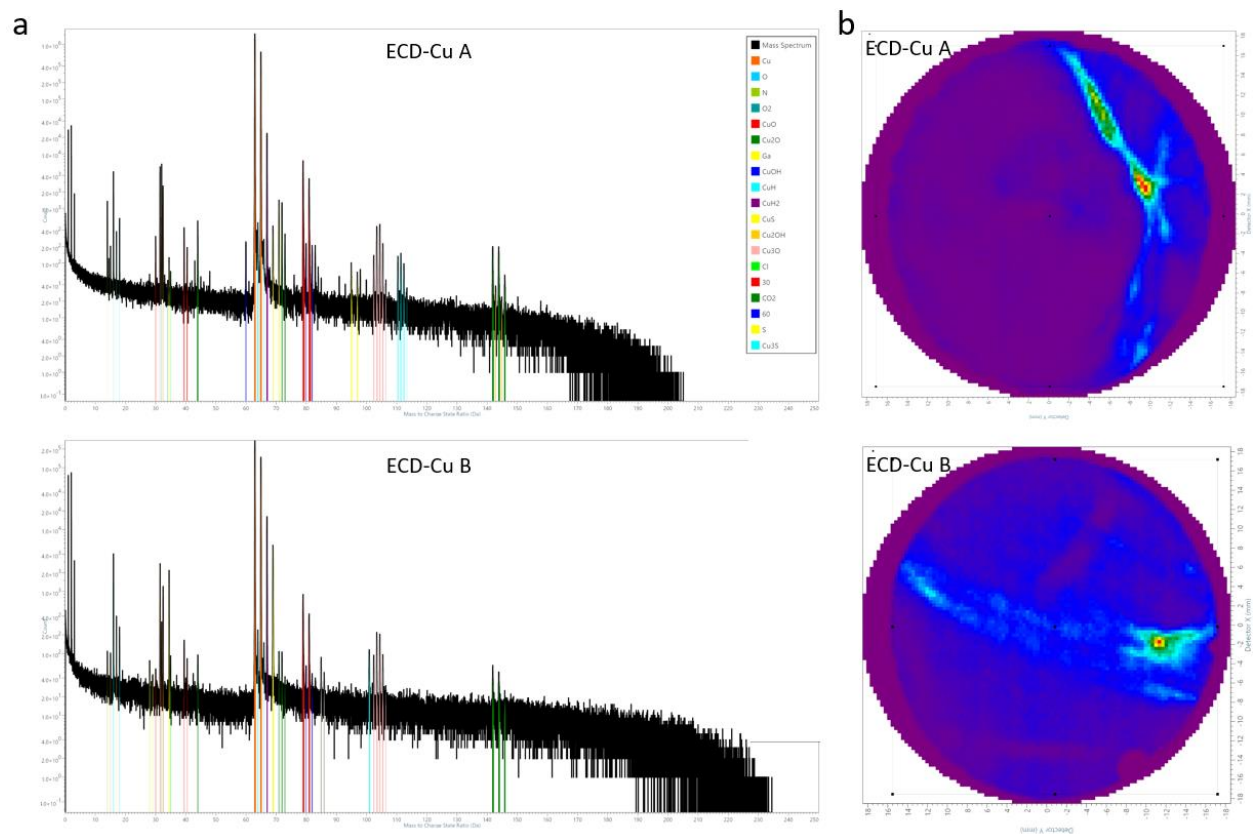
Supplementary Figure 1: The figure presents a comparative analysis of two machine learning approaches, Dictionary-based and Hough-based, by plotting their training and validation accuracy over 100 epochs. The x-axis represents number of epochs, while the y-axis denotes accuracy. Both methods display characteristic learning curves. The Dictionary-based model exhibits rapid progression in both training and validation accuracy, with the curves steeply rising and plateauing around 93% and 91%, respectively, by approximately the 30th epoch. In contrast, the Hough-based model demonstrates a more gradual increase, with convergence occurring near the 50th epoch and final training and validation accuracy stabilizing at approximately 81% and 79%. The vertical dashed lines at epochs 30 and 50 serve as visual markers for the points of convergence of the respective methods. Notably, in both approaches, the validation accuracy closely tracks the training accuracy throughout the epochs, reflecting consistent generalization performance and an absence of significant overfitting. This comparative visualization highlights the superior learning efficiency and final accuracy achieved by the Dictionary-based method relative to the Hough-based counterpart, offering valuable insights into their respective convergence rates and generalization abilities.



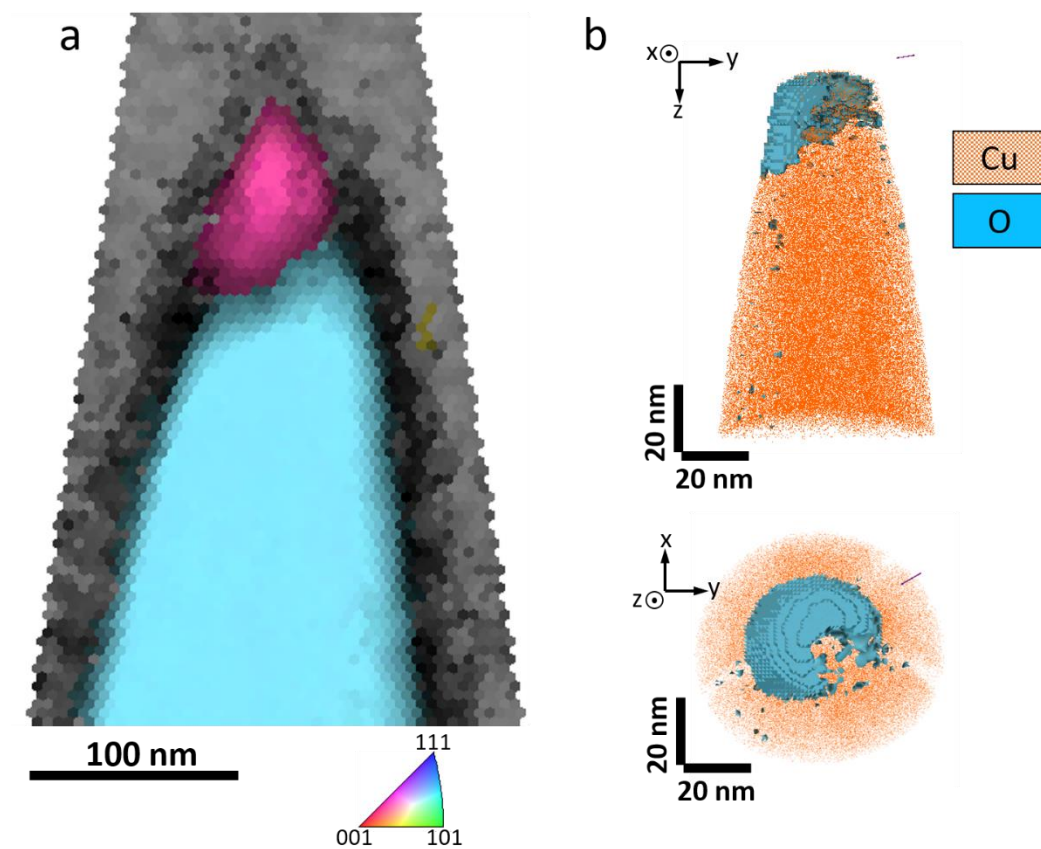
Supplementary Figure 2: The ML model is capable of generating detailed statistics for microstructural characterization parameters—including **a** grain density, **b** stresses, **c** strains, and **d** GND density, across different crystallographic orientations, as illustrated in the figure. This comprehensive data enables a deeper understanding of how orientation influences these properties.



Supplementary Figure 3: Preparation of APT-specimens from fs-laser half-grids of both thin-films. **a** Overview EBSD mappings of half-grids from thin-film A (top) and B (bottom). **b** EBSD mappings of single posts of thin-film A (top) and B (bottom). **c** FIB-micrographs showing the channelling contrast of Cu grains. Horizontal FIB-milled lines mark the grain boundaries that are prepared for the APT measurements in Fig. 5.



Supplementary Figure 4: a Mass spectra and **b** detector hit maps from the APT measurements of ECD-Cu A and B in Fig. 5. Grain boundaries are discernible in the detector hit maps due to their different evaporation behaviour.



Supplementary Figure 5: **a** Transmission Kikuchi diffraction (TKD) of an exemplary APT-specimen. Two grains are discernible **b** Front- and top-view of the APT reconstruction of the specimen in **a**. Cu is shown in orange and O iso-concentration surfaces in blue. The laser incidence direction is indicated by purple arrows. TKD leads to oxidation of the specimen tip.